

Magnetic Hyperthermia Using AMF and Nanoparticles

By

Duaa Al Esmael

April 20, 2020

A thesis Submitted to the Department of Physics

In Partial Fulfillment of Requirements for the Bachelor of Science

(Honours) in Medical Physics at Ryerson University

Dr. Carl Kumaradas

Abstract

Magnetic Hyperthermia is one of the promising cancer treatments that are under research when administrated alone or in combination with other treatments (Hainfeld & Huang, 2013). Superparamagnetic iron oxide nanoparticles (SIONPs) injected into tumor location and excited by applying an Alternating magnetic field (AMF) lead to heat generation in targeted tumor while sparing the healthy tissue leading to lower side effects. Several studies show that iron oxide nanoparticles(*ex. Fe₃O₃*) are suitable to be used in magnetic hyperthermia and approved to be safe for use on the human body (Rhythm R. *et al.*, 2016). In order for magnetic hyperthermia MH to be an effective treatment, several parameters need further investigation. Here we study the effect of increasing the applied magnetic field, as well as the effect of concentration and volume of MNPs. It was found that in order to avoid nonselective heating, it is important to keep the product of the applied magnetic field strength H and frequency f under a critical value found to be around $5 \times 10^9 \text{ kA/ms}$ which agrees with the reported value.

Acknowledgments

I would like to begin this section by expressing my gratitude to my supervisor, Dr. Carl Kumaradas for providing me the opportunity to work in this amazing project which I enjoyed. I would like also to thank my co-supervisor, Hisham Assi, for all the help and support through the fall and winter semesters.

Table of Contents

Abstract.....	ii
Acknowledgments.....	iii
Table of Contents.....	iv
List of Tables	vi
List of figures.....	vii
Symbols and Abbreviations.....	viii
Chapter 1: Introduction and Background.....	1
1.1 Basic Concepts of Magnetism	1
1.2 Hyperthermia	3
1.3 Magnetic Hyperthermia	5
1.3.1 Magnetic Nanoparticles	5
1.3.2 Mechanisms of Heat Generation inside an AMF.....	5
1.3.2.1 Relaxation Mechanisms	6
1.3.2.2 Power loss in MNPs.....	9
1.3.2.3 Eddy Currents Heating.....	10
1.4 Objectives and aims	11
Chapter 2: Materials and Methods.....	12
Chapter 3: Results	16
3.1 Effect of Current on Temperature Rise.....	16
3.2 Effect of MNP Concentration on Temperature Rise.....	19
3.3 Effect of MNP volume on Temperature Rise	22
3.4 Trial with Optimal parameters	23
3.5 Control Heating.....	24
3.6 Heating below the center of the loop	25

Chapter 4: Discussion	26
4.1 Recommendations.....	27
Chapter 5: Conclusion and Future studies	29
Chapter 6: References	30

List of Tables

Table 1: current applied and the calculated magnetic field strength.....	14
Table 2: Summary of the results for current effect on heat generation.....	18
Table 3: Summary of the results for effect of MNP Concentration on temperature change.	22
Table 4: summary of the results for the trial with optimal parameters	23

List of figures

Figure 1: Hysteresis loop for ferri/ferromagnetic particles (Estelrich et al., 2015)	2
Figure 2: single domain size and superparamagnetic size for different materials (Krishnan et al., 2006)	3
Figure 3: Effect of anisotropy constant K on relaxation time τ . Obtained from (Deatsch and Evans, 2014)	9
Figure 4: Magnetization Curve for 20 nm SIONPs	12
Figure 5: Heat and Power station.....	13
Figure 6: Lutron connected to the computer.....	13
Figure 7: MNP injection	14
Figure 8: AMF heating in tissue with 25 ul MNP injection and different current. In all figures, I_{rms} is the root mean square current and N is the number of trials.....	17
Figure 9: AMF Heating in tissue with no MNP injection and different I_{rms}	17
Figure 10: Difference in T of tissue heating after 15 min.....	17
Figure 11: Therapeutic ratio (R) currents 5 to 25A, respectively (change in T for heating tissue with 25 ul MNP injection (20 mg/ml) divided by change in T for tissue with no MNP injection.	18
Figure 12: AMF heating in tissue with 25 ul MNP injection (5mg/ml) and different I_{rms}	19
Figure 13: MNP concentration effect on temperature rise with 5 A	19
Figure 14: MNP concentration effect on temperature rise with 10 A.....	20
Figure 15: MNP concentration effect on temperature rise with 15 A.....	20
Figure 16: MNP concentration effect on temperature rise with 20 A.....	21
Figure 17: MNP concentration effect on temperature rise with 25 A.....	21
Figure 18: effect of increasing the MNP volume from 25 ul to 50 ul with 5, 10 and 25 A.....	22
Figure 19: AMF heating in tissue with zero MNP injection and with 20 ul MNP injection (20 mg/ml).....	23

Symbols and Abbreviations

AMF- Alternating magnetic field

MH- Magnetic hyperthermia

MNP- Magnetic Nanoparticles

SIONP- Superparamagnetic iron oxide nanoparticles

H- Magnetic field strength

f- frequency

Chapter 1: Introduction and Background

According to the world health and organization, Cancer is considered to be a serious health problem and is the second dominant cause of death worldwide. The number of death due to cancer is predicted to be 82,100 from 220,400 new cancer diagnoses in Canada in 2019, according to Canadian Cancer Society. As cancer plays an important role in public health and affects the mortality rate, researches around the world focus on optimizing cancer treatment. Surgery, Chemotherapy and Radiation therapy are the common current cancer treatments that can be given separately or in combination depending on several factors such as cancer stage and location. Even though certain types of cancers can be cured with the current technologies, harmful side effects are seen in the patients due to the damage of their health tissues. As a result, treatment that cures various types of cancers at different locations and reduces the side effect is needed in order to raise the survival rate as well as improving patient's quality of life.

1.1 Basic Concepts of Magnetism

Materials can be classified based on their response to an applied magnetic field (H) depending on their magnetic susceptibility (χ), the magnetic induction (B) is given by

$$B = \mu_0(M + H) \quad (1)$$

$$M = \chi H \quad (2)$$

Where μ_0 is the permeability of free space, and M is the magnetization of the material equal to the magnetic moment (m) per unit volume (V).

Diamagnetic materials with a small and negative χ will show a weak magnetization and in the opposite direction of the applied field. Paramagnetic materials with small and positive χ will also lead to a weak magnetization but in a parallel direction with the applied field (Spaldin, 1991; Jiles,

1991). Both have no magnetic properties upon the removal of the magnetic field (MF). Ferromagnetic materials where domain walls separate parallel magnetic moments have a net magnetization even in the absence of an external MF (Spaldin, 1991). When they are heated below their Curie temperature T_C , they will be magnetized up to the saturation magnetization (M_s) and will have remanence magnetization (M_r) when the applied field is removed which can be seen in the M-H curve (hysteresis loop) in Figure 1 (Estelrich *et al.*, 2015; Pankhurst *et al.*, 2003). Similar characteristic is seen in ferrimagnetic materials where the magnetic moments align antiparallel and with different magnitude in each domain.

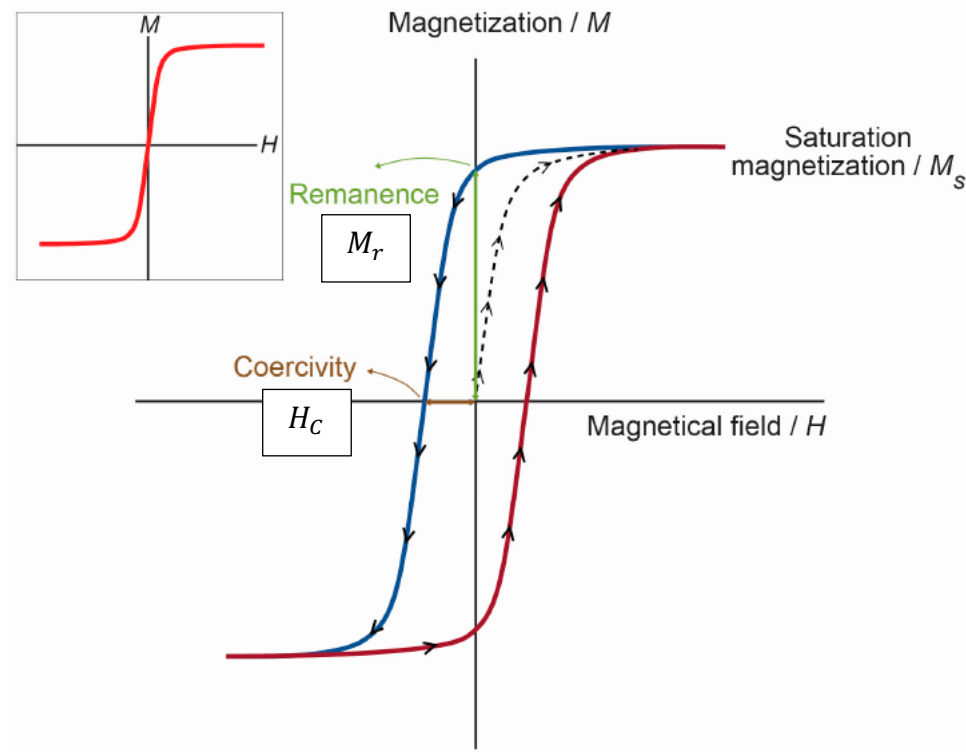


Figure 1: Hysteresis loop for ferri/ferromagnetic particles. Obtained from (Estelrich *et al.*, 2015)

When the size of particles decreases to a few nanometers, they become single-domain magnetic nanoparticles. With a further decrease in size, they will present superparamagnetic behavior, meaning that they can be magnetized up to their saturation and have no remaining magnetization

upon the removal of the MF (Wang and Wang*, 2004). Figure 2 shows the single domain size D_{crit} and the superparamagnetic size D_{sp} for some ferromagnetic materials.

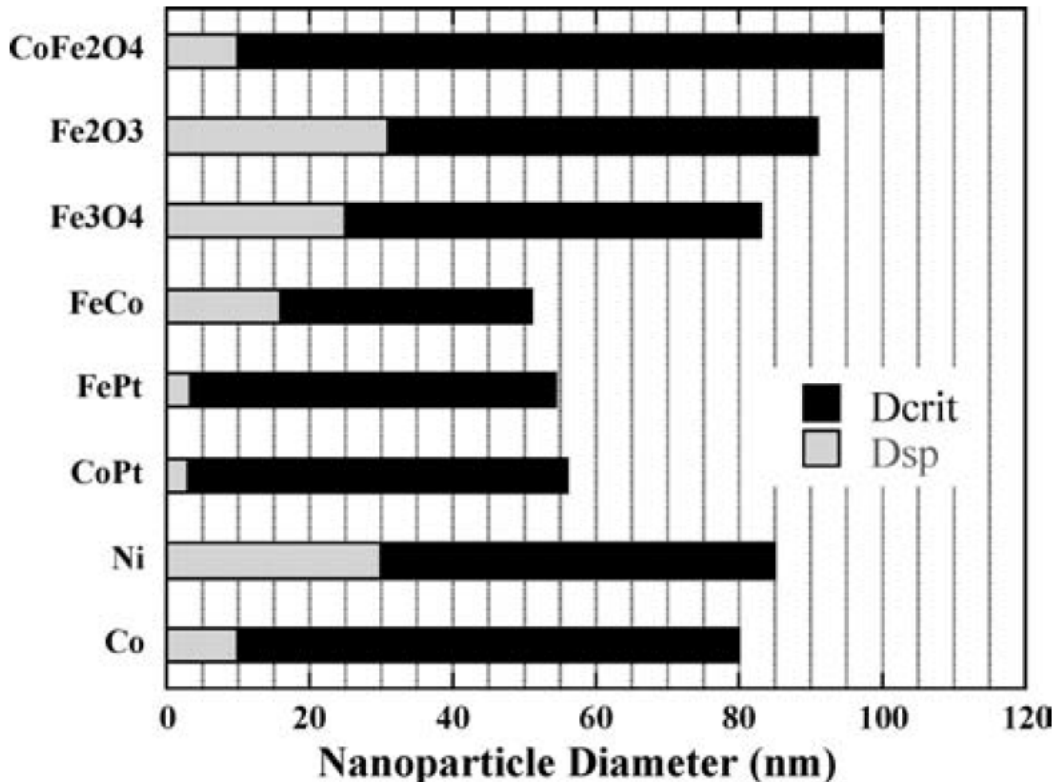


Figure 2: single domain size and superparamagnetic size for different materials. Obtained from (Krishnan et al., 2006)

1.2 Hyperthermia

Hyperthermia treatment aims to achieve a desired therapeutic effect using heat to elevate the temperature of the whole-body or specific region of the body up to 41 to 45°C for a defined period. Hyperthermia as a cancer therapy has a long history started around 3000 B.C. In ancient Greece and Rome researchers believe that all diseases can be treated using heat. The interest in modern

hyperthermia was started again in 1975 when an international congress on Cancer therapy by Hyperthermia and Radiation was held in Washington, D.C. (USA) (Gas, 2011). Both malignant and non-malignant cells are sensitive to increase in temperatures; however, malignant cells are more sensitive to heat due to their hypoxic and acidic microenvironment (van der Zee, 2002). Unlike healthy tissue, tumor tissue has a heterogeneous vascular structure leading to difficulty in releasing the excess amount of heat due to the low blood flow rate (Reitan *et al.*, 2010; Suriyanto, Ng and Kumar, 2017). As a result of tissue heating, the blood flow rate will be dramatically increased in healthy tissue that can be up to 20 times more than before heating, whereas a very slight increase might occur in tumor tissue (Song *et al.*, 1984; Suriyanto, Ng and Kumar, 2017). Depending on the temperature and treatment time, hyperthermia can cause cytotoxic effects leading to a cancerous cell death by apoptosis based on proteins denaturation (van der Zee, 2002). Moreover, hyperthermia can lead to indirect cell death by increasing the susceptibility toward conventional cancer therapies such as radiotherapy and some chemotherapeutic drugs. Applying heat to the tumor area will lead to better drug delivery as a result of doubling the blood flow as well as increasing tumor radiosensitivity due to increased oxygen concentration (Hegyi, Szigeti and Szász, 2013). Furthermore, hyperthermia can enhance the result of radiotherapy by preventing the mechanism of DNA damage repair (Suriyanto, Ng and Kumar, 2017).

There are three main categories of hyperthermia: whole-body hyperthermia (WBH), regional hyperthermia (RH), and localized hyperthermia. WBH is the oldest method; however, in order to lower the amount of the side effects results from non-specific heating, RH, and localized hyperthermia were used (Wust *et al.*, 1994).

1.3 Magnetic Hyperthermia

Magnetic hyperthermia is one of the promising cancer treatments where magnetic nanoparticles (MNPs) in superparamagnetic size are administrated to the tumor location and then exposed to an AMF. This will lead to tumor regression as a result of converting the electromagnetic energy into heat, and then heat dissipation into the tumor (Jeyadevan, 2010).

1.3.1 Magnetic Nanoparticles

The development of the nanotechnology field allows the use of nanoparticles in medical applications due to their unique physical and chemical properties (Pankhurst, 2006). The small size of nanoparticles (<100 nm) allows them to be compatible with a range of biological molecules, and thus detection and therapy of diseases can be improved (Pankhurst, 2006). Among the different types of nanoparticles, magnetic nanoparticles, especially superparamagnetic iron oxide nanoparticles (SIONPs), are widely studied to be used in medical applications. They can be used in magnetic resonance imaging MRI as contrast agents, drug and gene delivery, and in magnet hyperthermia for cancer treatment. Magnetite (Fe_3O_4) and maghemite (γFe_3O_4) iron oxide NPs are favorable to be used in MH due to their biocompatibility and colloidal stability (Wang and Wang*, 2004). Also, their surface can be modified to help their localization inside the tumor. They are approved by the US Food and Drug Administration (FDA) and European Medicines Agency (EMA) to be safe for human use (Colombo *et al.*, 2012).

1.3.2 Mechanisms of Heat Generation inside an AMF

Using a high frequency alternating magnetic field in magnetic hyperthermia leads to heat generation due to several mechanisms. The dominant mechanism can be determined based on

several factors, including the properties of the exposed material, as well as the strength and frequency of the applied field (Glöckl *et al.*, 2006).

When MNPs are exposed to an AMF, the electromagnetic energy of the MNPs will be converted into thermal energy. The production of heat can be explained by hysteresis loss, Néel, and Brownian relaxations depending on the size of MNP (Deatsch and Evans, 2014). The hysteresis loss is responsible for heating multi-domain ferro/ferrimagnetic nanoparticles. However, the relaxation mechanisms are responsible for heating single-domain superparamagnetic nanoparticles (Deatsch and Evans, 2014; Glöckl *et al.*, 2006). Thus, the hysteresis loss is negligible in MH since the since the particle used are superparamagnetic.

1.3.2.1 Relaxation Mechanisms

The magnetic anisotropy energy of SIONPs that keeps their magnetic moments in a specific direction is given by

$$E = KV \sin^2 \theta \quad (3)$$

Where K is the anisotropy constant and V is the volume of the particle.

SIONPs have a small anisotropy energy due to their small size and as a result, the energy barrier (KV) that needs to be overcome to switch between two states is small comparing to the thermal energy ($k_B T$), k_B is the Boltzmann constant .

The mechanism of heat generation in single domain SIONPs was studied by Rosensweig. He assumed that only rotational relaxation is responsible for heating, and the relationship between magnetization (M) of a particle and the applied magnetic field (H) is linearly proportional. In ferrofluid, smaller SIONPs will undergo Néel relaxation, which is rotation and alignment of the magnetic moment within the particle with the applied magnetic field while the particle itself is

stationary. Upon the removal of the applied field, heat will be dissipated due to a delay in relaxation of the magnetic moment to equilibrium state simultaneously with the field caused by a resistance of this reorientation. Besides Néel relaxation, larger SIONPs and single-domain ferromagnetic NPs will undergo Brownian relaxation. The physical rotation of the particle occurs while the magnetic moment is fixed along the easy axis. Once the field is removed, heat is generated due to friction caused by the particle's rotation inside a medium (2011; Li, Hodgins and Peterson, 2011; Jeyadevan, 2010; Rosensweig, 2002).

The following equations express Néel relaxation time (τ_N) and Brownian relaxation time τ_B

$$\tau_N = \frac{\tau_0\sqrt{\pi}}{2} \frac{\exp(\Gamma)}{\sqrt{\Gamma}} \quad (4)$$

$$\tau_B = \left(\frac{3\eta V_H}{k_B T} \right) \quad (5)$$

Where τ_0 is a constant called the attempt time, which is characteristic for the material and is estimated to be around 10^{-9} s , k_B is the Boltzmann constant, T is the temperature, η is the viscosity of the medium and V_H is the hydrodynamic particle volume (Demas and Lowery, 2011; Li, Hodgins and Peterson, 2011; Jeyadevan, 2010; Rosensweig, 2002).

Unlike Néel relaxation, where its contribution to heating is only affected by MNP properties, contribution to heating through Brownian relaxation is affected by the surrounding medium. If the medium has a high viscosity, then the heat dissipation through Brownian mechanism will be decreased (Jeyadevan, 2010). Both mechanisms are combined by the effective relaxation time dominated by the faster mechanism, which has a shorter relaxation time. The effective relaxation time is given by:

$$\tau = \frac{\tau_N \tau_B}{\tau_N + \tau_B} \quad (6)$$

The size distribution in magnetic fluid affects the relative contribution of each mechanism (Jeyadevan, 2010). The contribution of each mechanism depends on the size of the SIONP, where there is a critical diameter for the transition from Néel relaxation to Brownian relaxation. At this diameter, both mechanisms will contribute to heating (Parmar *et al.*, 2015). Different studies show a different value of the critical diameter due to its dependence on the medium viscosity and anisotropy constant (K), where K is affected by the crystal structure, shape, and surface of the particle (Glöckl *et al.*, 2006; Ondeck *et al.*, 2009). Figure 3 shows the critical diameter for transition between the two relaxation mechanisms, and relaxation times for various anisotropy constants in iron oxide nanoparticles. It is obvious that as the anisotropy constant increases, the critical diameter decreases (Deatsch and Evans, 2014). Another study for magnetite nanoparticles (Fe_3O_4) suspended in water with $K = 8 \text{ kJ/m}^3$; the critical diameter was 20 nm (Li, Hodgins and Peterson, 2011). Rosensweig (2002), studied the effect of different viscosity values on the heating rate and it was concluded that the heating rate increases as the viscosity value decreases. Thus, Brownian relaxation may not contribute to heating in biological tissue (Hergt *et al.*, 1998). Dutz *et al.* (2011) performed an experiment where maghemite NPs with a diameter of 14 nm were injected in tumor tissue and exposed to an alternating magnetic field ($H=25 \text{ kA/m}$, $f= 400 \text{ kHz}$). The result shows that only Neel relaxation contribute to heating and Brownian relaxation is suppressed due the inability of the particle movement inside the tumor (Dutz *et al.*, 2011; Dutz and Hergt, 2014).

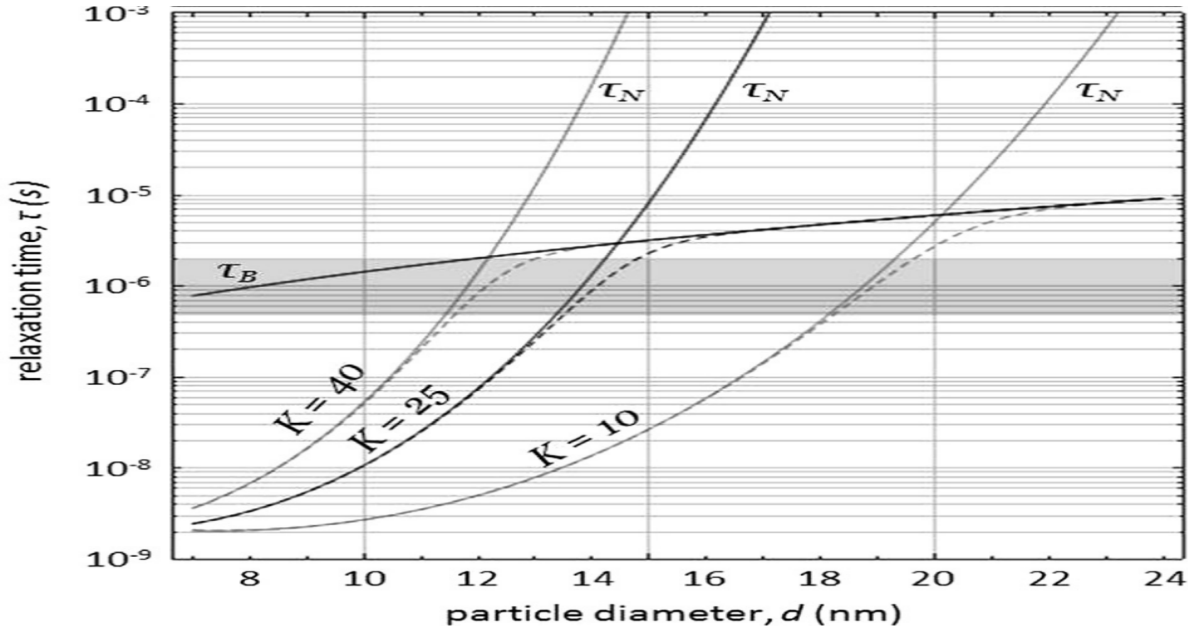


Figure 3: Effect of anisotropy constant K on relaxation time τ . Obtained from (Deatsch and Evans, 2014)

1.3.2.2 Power loss in MNPs

The volumetric power dissipation (p), specific absorption rate (SAR), in superparamagnetic NPs was derived by Rosensweig as:

$$P = \frac{1}{2} \mu_0 x_0 H^2 \omega \frac{\omega\tau}{1+\omega^2\tau^2} \quad (7)$$

$$x_0 = x_i \frac{3}{\xi} (\coth \xi - \frac{1}{\xi}) \quad (8)$$

Where $\omega = 2\pi f$, f is the frequency, x_0 is the static susceptibility, x_i is the initial and the Langevin parameter $\xi = \frac{\mu_0 M_s H V}{K_B T}$ (Deatsch and Evans, 2014; Rosensweig, 2002; Zhang, Gu and Wang, 2007).

According to Rosensweig model, heat generation in superparamagnetic NPs depends on the square of the magnetic field strength H; however, changing the value of $\omega\tau$ gives different cases (Hergt *et al.*, 2006; Deatsch and Evans, 2014). Maximum P occurs when $\omega\tau = 1$ and thus frequency can

be adjusted to get maximum power dissipation (Deatsch and Evans, 2014). At low frequency ($\omega\tau \ll 1$), P depends on the square of the frequency, and at high frequency ($\omega\tau \gg 1$), P becomes independent of the frequency (Hergt *et al.*, 2006; Deatsch and Evans, 2014). Power dissipation is also affected by magnetic NPs priorities; as a result, studies reported various maximum SAR with different MNP sizes (Zhang, Gu and Wang, 2007). An experiment was done by Ma *et al.*, with different sizes of magnetite NPs dispersed in water and exposed to (80 kHz, 32.5 kA/m). The result particles with a diameter of 46 nm have the highest SAR (Ma *et al.*, 2004; Zhang, Gu and Wang, 2007). Another experiment shows that the highest SAR falls between 12 to 20 nm for SIONPs (Deatsch and Evans, 2014). It was also found that size distortion and preparation methods with different coating lead to the variation on reported SAR (Deatsch and Evans, 2014; Zhang, Gu and Wang, 2007).

1.3.2.3 Eddy Currents Heating

AMF generating system produces both electric and magnetic fields where the electric field could induce eddy currents that generate heat when passing through a material (Stigliano *et al.*, 2016). The strength of the eddy currents heating mechanism can be demonstrated by rate of heat production per tissue volume which depends on the diameter and electrical conductivity (σ_t) of the exposed material as well as the frequency and amplitude of the applied magnetic field (Atkinson, Brezovich and Chakraborty, 1984; Kozissnik *et al.*, 2013)

$$P_{eddy} = \sigma_t (\pi \mu_0)^2 (Hf)^2 r^2 \quad (9)$$

Where σ_t r is the radius of the material.

In the case of magnetic hyperthermia, the MNPs themselves are not able to induce eddy currents due to their small size, as well as their poor electrical conductivity. However, the biological tissue

has a high electrical conductivity that can induce eddy currents under an AMF resulting in non-specific heating of both healthy and tumor tissues (Glöckl *et al.*, 2006; Salunkhe, Khot and Pawar, 2014). In order to avoid undesirable heating in healthy tissue, it was recommended that the product of the applied magnetic field strength and frequency (Hf) should be limited in humans. The limit was found experimentally by Atkinson et al., who studies the effect of applying AMF for more than one hour at a region with a diameter of 30 cm in many patients. He recommended that the limit should not exceed the value $4.85 \times 10^8 A/ms$ (Atkinson, Brezovich and Chakraborty, 1984; Hergt and Dutz, 2007) . Other studies show that the limit varies from 4.5×10^8 to $8.5 \times 10^8 A/ms$ depending on the exposed area (Stigliano *et al.*, 2016). Later, Hergt et al., suggested that depending on the seriousness of the disease and for a smaller exposed region, the limit may be increased to $5 \times 10^9 A/ms$ (Hergt & Dutz, 2007).

1.4 Objectives and aims

Magnetic hyperthermia is a promising treatment where it is possible to generate heat only at the targeted area leading to cancer cells death. In order to have selective heating, it is important to understand the effect of AMF parameters and MNP properties.

The study aims to optimize the magnetic hyperthermia treatment by studying the effect of different parameters on heat generation over time.

The specific aims were to 1/ find the optimal AMF parameters; specifically finding the optimal magnetic field strength H , while the frequency f is fixed, by applying different currents I and determining the optimal one, 2/ study the effect of injecting MNPs with different concentrations and volumes in tissue, 3/ evaluate the possibility of control heating; and 4/ finding the possible biophysical limitations.

Chapter 2: Materials and Methods

Iron oxide MNPs (Fe_3O_4) with a diameter of 20 nm with PVP surface coating from nanoComposix were used in all conducted experiments. The particles show a superparamagnetic behavior at room temperature as shown in the following figure.

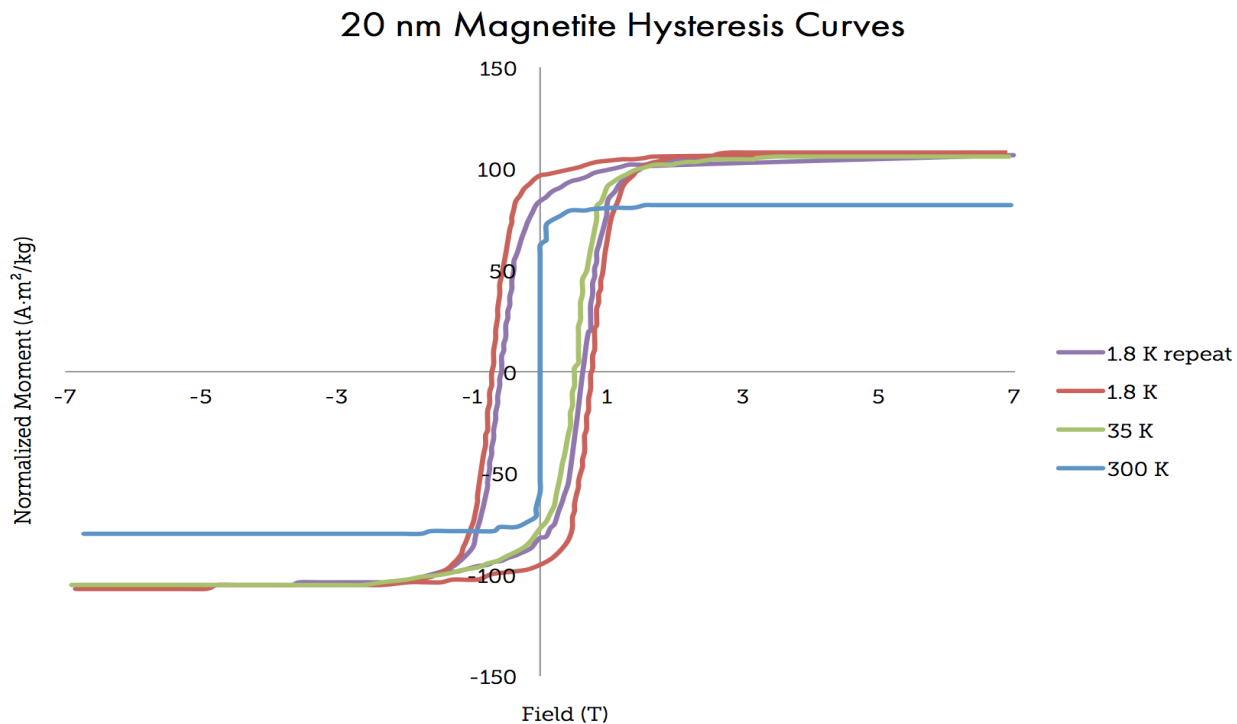


Figure 4: Magnetization Curve for 20 nm SIONPs. Obtained from (Nanocomposix.eu, 2020).

Induction heating system used consist of 5 kW power supply connected to heat station has a two-turn induction coil with an inner diameter of 4.8 cm. (UltraHeat UPT-W8, Ultraflex Power Technologies, New York, NY) and (R2200V Fan, Dynaflux, Cartersville, GA) are the instruments model numbers.

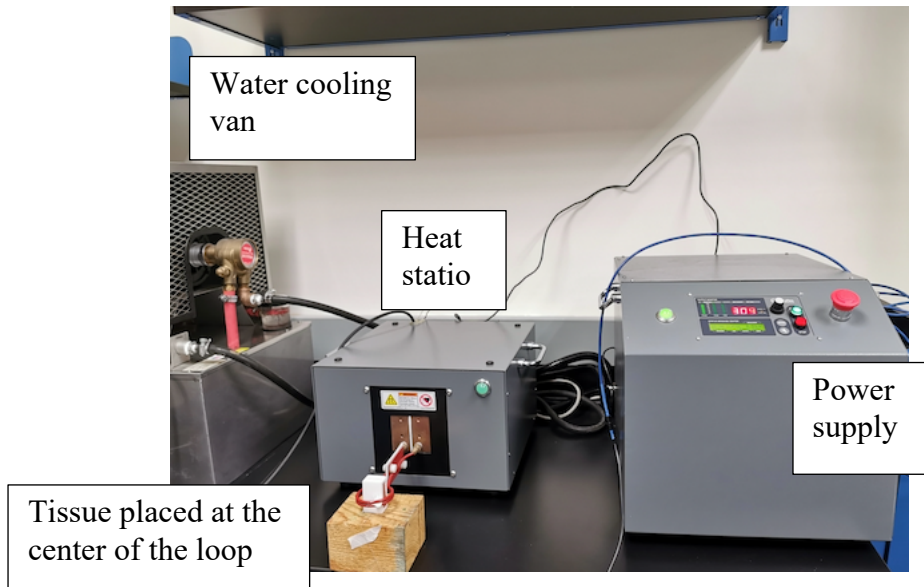


Figure 5: Heat and Power station

Luxtron (3100) Fluoroptic Thermometer with fiber optic was used to measure the temperature where it is connected to the MATLAB program to save the results.

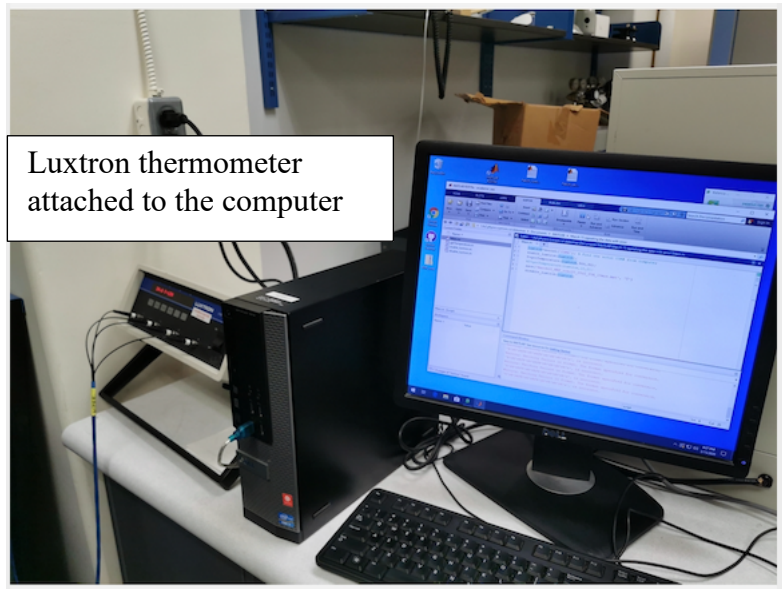


Figure 6: Luxtron Fluoroptic Thermometer connected to the computer

MNPs were injected in tissue using syringe pump with syringe as shown in the following figure.

The rate of injection was 2 μ l/min.



Figure 7: MNP injection

Pork meat was chosen as tissue sample used in all experiments.

Magnetic nanoparticles with a diameter around 5 nm was first heated alone to determine their ability to get heated. Particles did not show any increase in temperature. Thus 20 nm SIONPs were used in all experiments after determining their ability to get heated with different currents. All the current shown in the discussion and figures are the applied current in root mean square. The field strength H was calculated by finding the peak current and multiplying it by a transformer ratio (1:20). The frequency applied in all experiments is fixed ($f=394\text{kA/m}$), while the magnetic field strength was adjusted changed by changing the current from the machine.

Table 1: current applied and the calculated magnetic field strength

Current, I rms (A)	H (kA/m)
25	29.5

20	23.6
15	17.7
10	11.8
5	5.8

AMF heating in tissue was performed with 1/ no MNP injection, 2/ 25 ul MNP injection (20 mg/ml), 3/ 25 ul MNP injection (5 mg/ml), 4/ 50 ul MNP injection (20 mg/ml), and 4/ 20 ul MNP injection (20 mg/ml) with different current.

Two trials for control heating were performed where the first trial, 14.7A and 12.2 A was applied, respectively, each for 20 min. The second trial was done with 25A, 18.5A and 12.2 A each for 10 min, respectively.

Last experiment, AMF heating 1.2 cm below the center of the loop was done with 0 MNP injection and 50 ul MNP injection (20 mg/ml).

Chapter 3: Results

The results are presented in six sections. Section 3.1 shows the effect of increasing the current in temperature rise where figures 8 shows the temperature rise in tissue with 25 μl MNP injection and figure 9 shows the temperature rise in tissue with no MNP injection. Figure 11 shows the therapeutic ratio R_1 to R_5 for the used currents 5 to 25 A, respectively. Section 3.2 shows the effect of changing the concentration of MNPs on temperature rise presented in figure 12. figures 13 to 17 are plotted to compare the temperature change with different MNP concentration at each current. The effect of increasing MNP volume in heat generation is presented in section 3.3. section 3.4 shows the result of an experiment under parameters selected to be on the optimal range. Two trials for control heating are presented in section 3.5 and finally, result for AMF heating below the center of the loop is presented in section 3.6. Tables at the end of each section summarize the final results where the final change in temperature is presented.

3.1 Effect of Current on Temperature Rise

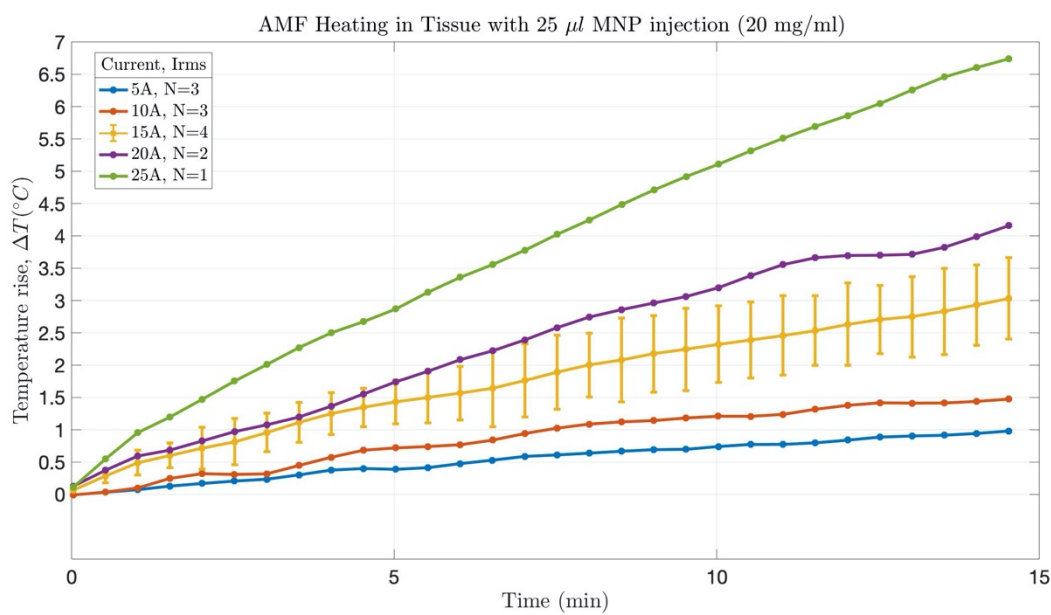


Figure 8: AMF heating in tissue with 25 μ l MNP injection and different current. In all figures, I_{rms} is the root mean square current and N is the number of trials.

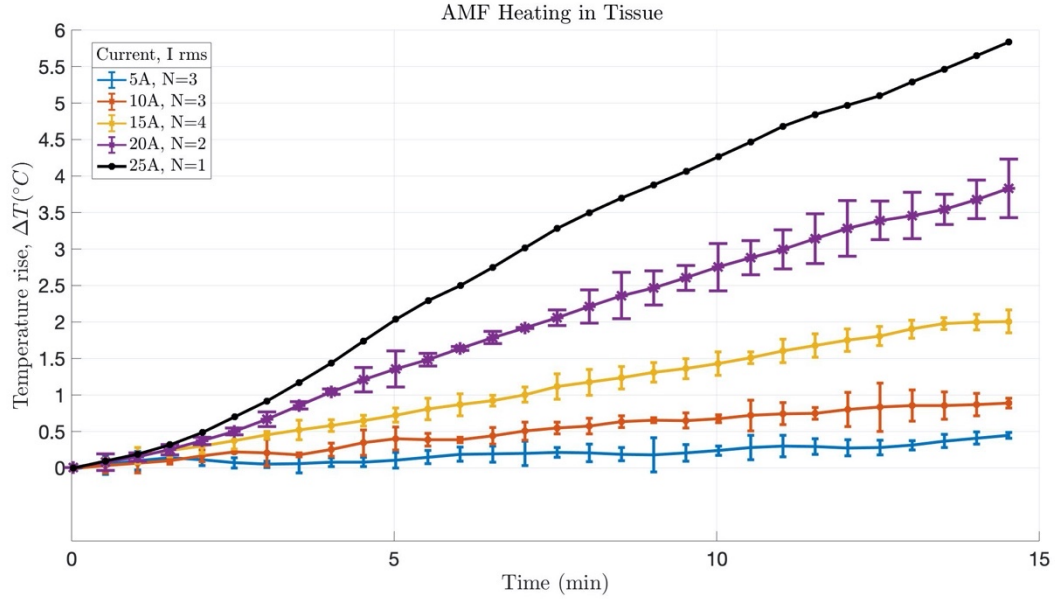


Figure 9: AMF Heating in tissue with no MNP injection and different Irms.

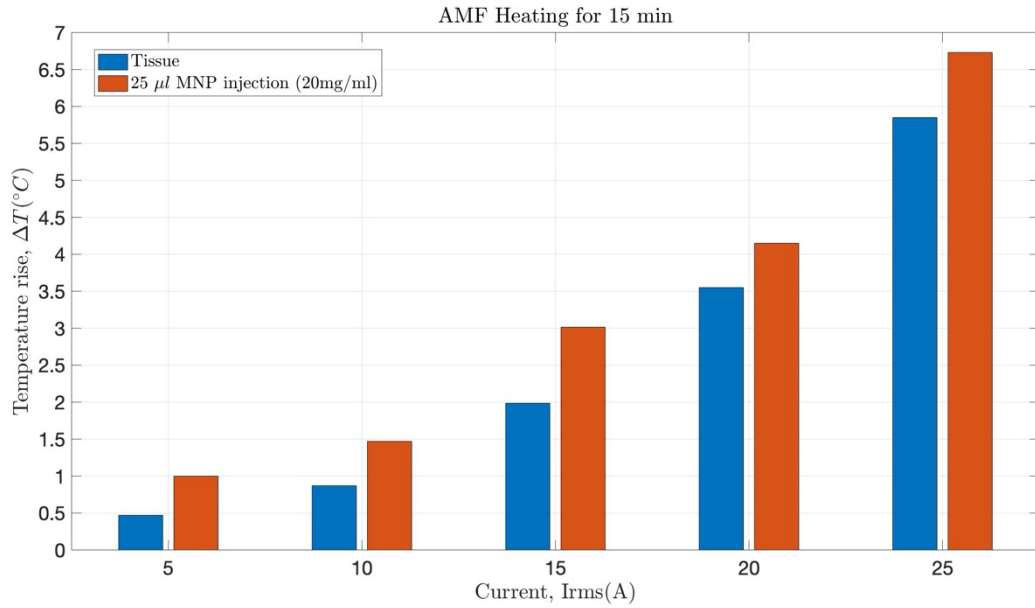


Figure 10: Difference in T of tissue heating after 15 min.

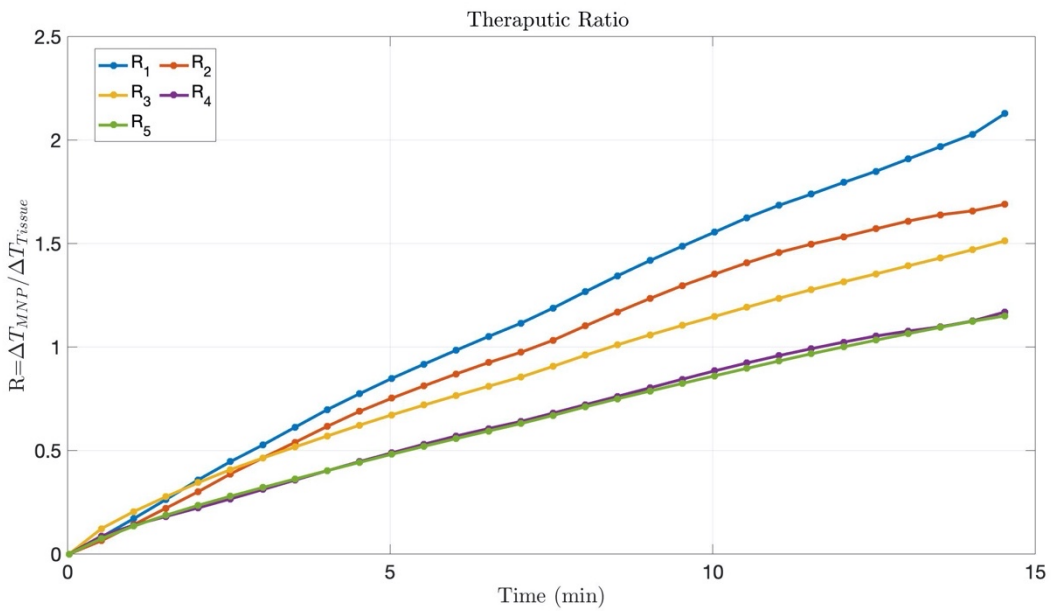


Figure 11: Therapeutic ratio (R) currents 5 to 25A, respectively (change in T for heating tissue with 25 ul MNP injection (20 mg/ml) divided by change in T for tissue with no MNP injection.

Table 2: Summary of the results for current effect on heat generation

I_{rms} (A)	ΔT_{Tissue}	ΔT_{MNP}	R
		25 ul (20 mg/ml)	
5	0.47°C	1°C	2.12
10	0.87°C	1.47°C	1.68
15	1.98°C	3.01°C	1.52
20	3.55°C	4.15°C	1.16
25	5.7°C	6.73°C	1.18

3.2 Effect of MNP Concentration on Temperature Rise

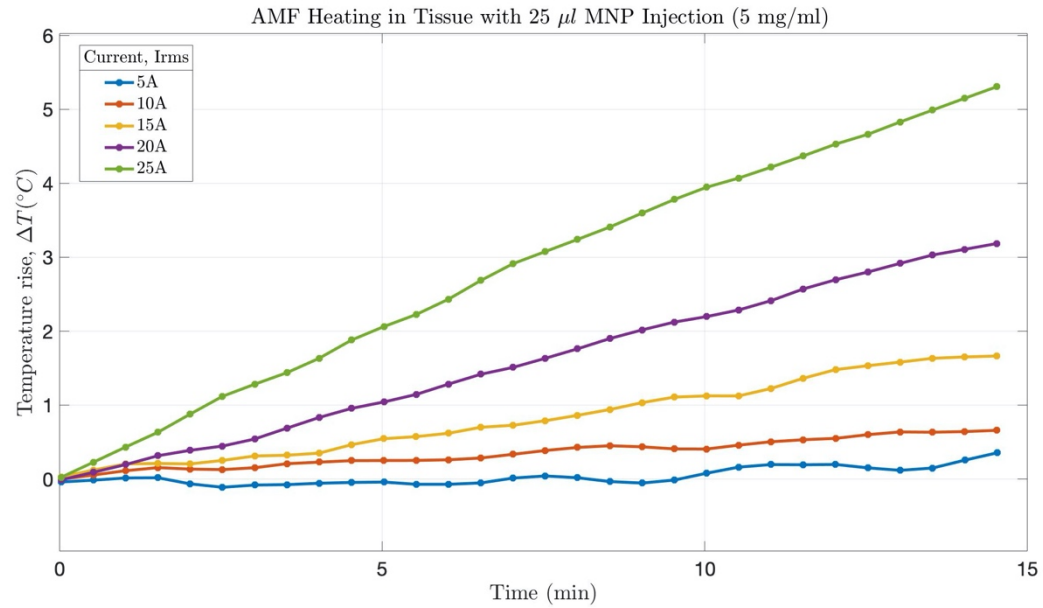


Figure 12: AMF heating in tissue with 25 μl MNP injection (5mg/ml) and different Irms.

The following figures were plotted to compare the results of heating tissue with different MNP concentrations at different current.

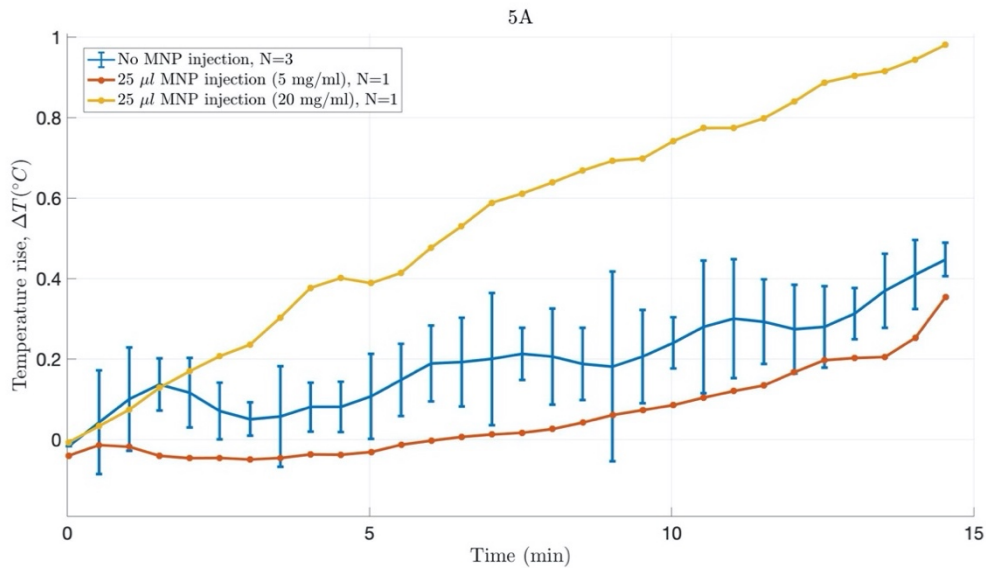


Figure 13: MNP concentration effect on temperature rise with 5 A

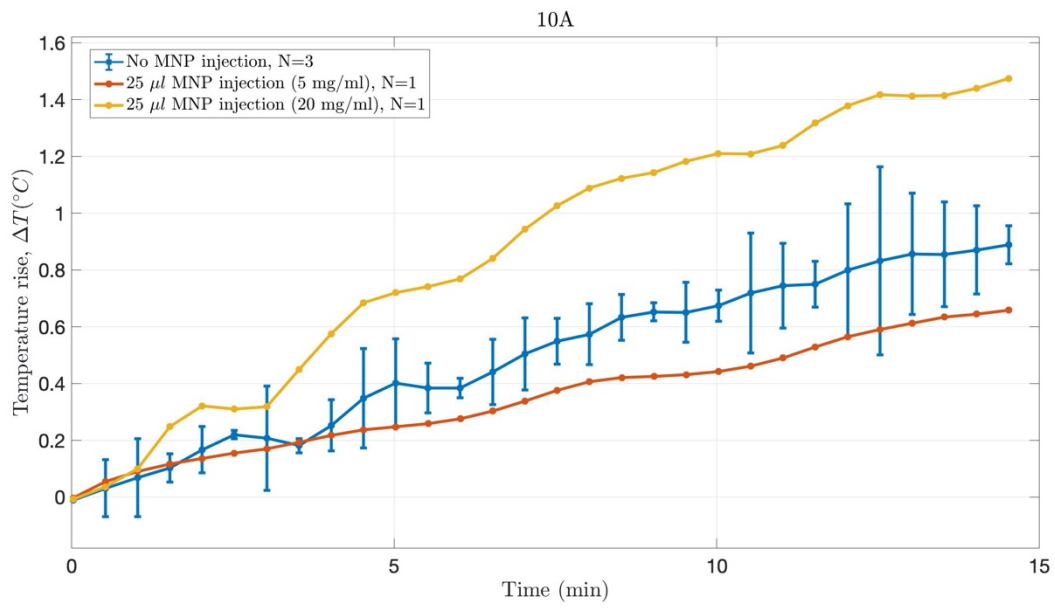


Figure 14: MNP concentration effect on temperature rise with 10 A

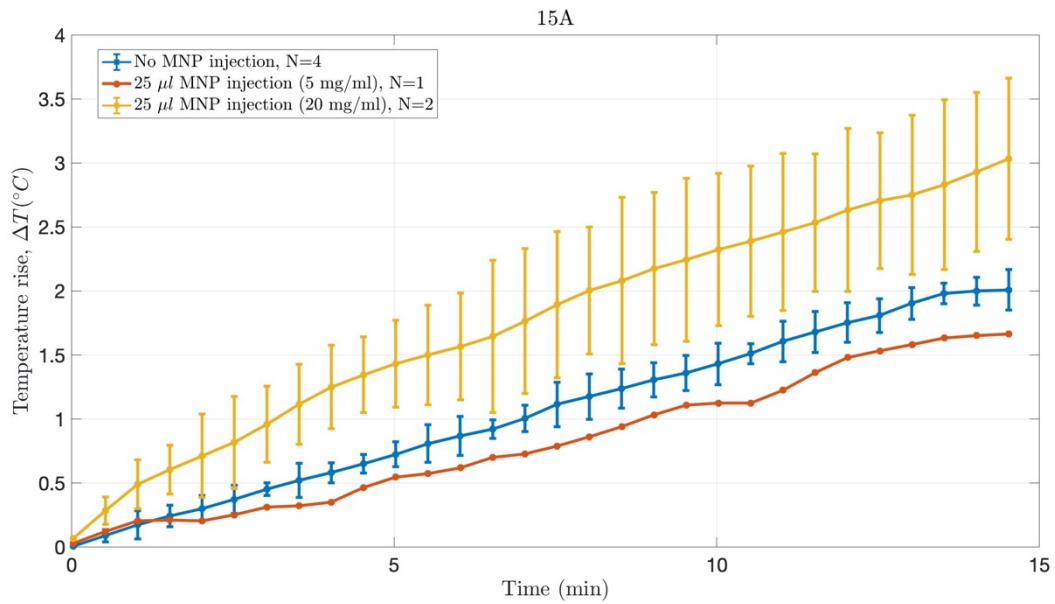


Figure 15: MNP concentration effect on temperature rise with 15 A

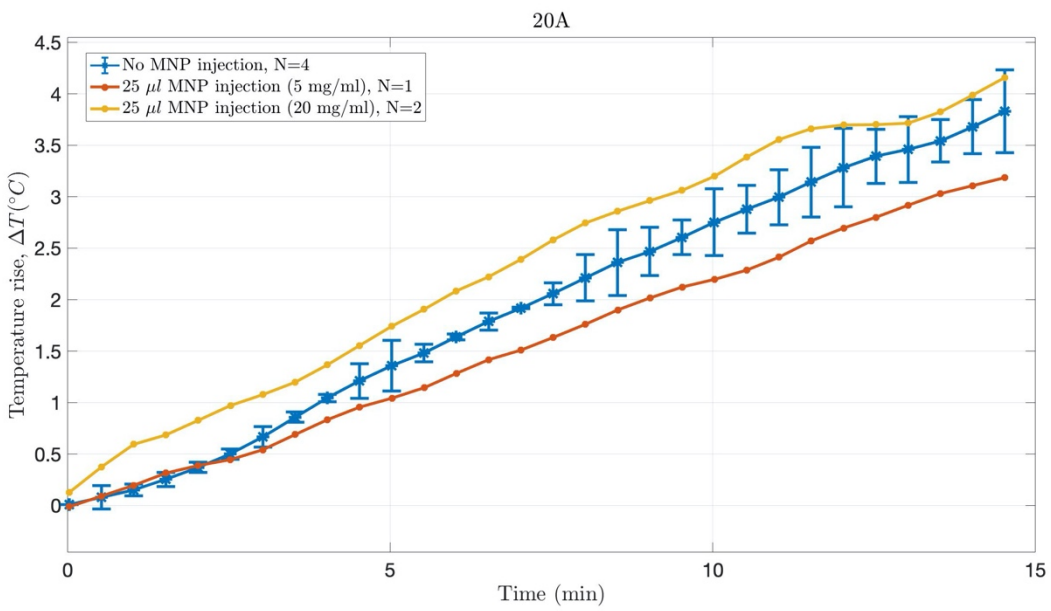


Figure 16: MNP concentration effect on temperature rise with 20 A

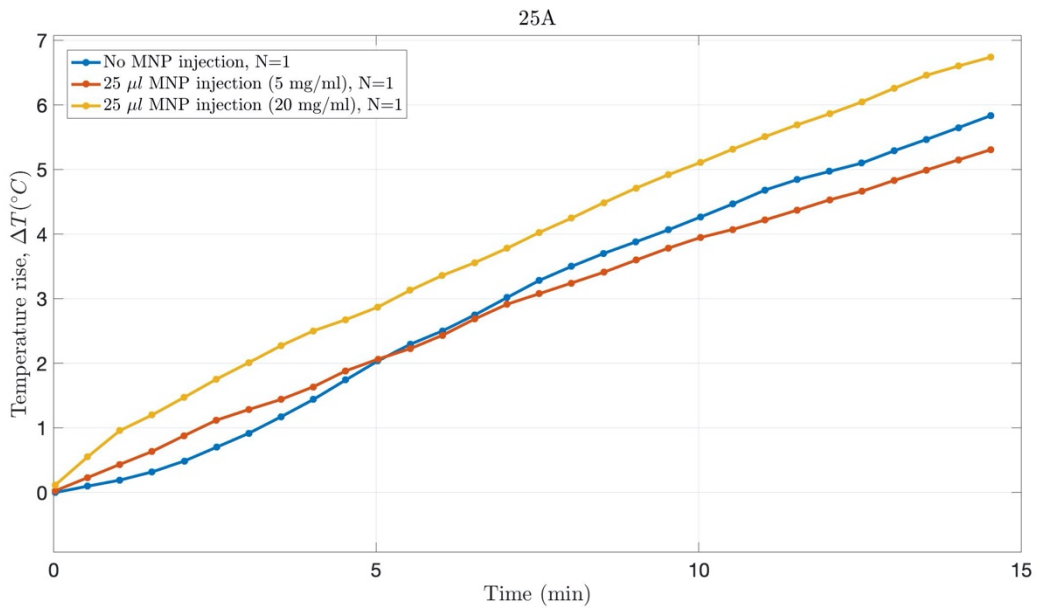


Figure 17: MNP concentration effect on temperature rise with 25 A

Table 3: Summary of the results for effect of MNP Concentration on temperature change.

I_{rms} (A)	ΔT_{Tisse}	ΔT_{MNP}	ΔT_{MNP}
		25 ul, (5 mg/ml)	25 ul, (20 mg/ml)
5 A	0.47 °C	0.34 °C	1.0
10 A	0.87 °C	0.65 °C	1.5
15 A	1.98 °C	1.6 °C	3
20 A	3.55 °C	3.2°C	4.2
25 A	5.7 °C	5.9°C	6.8

3.3 Effect of MNP volume on Temperature Rise

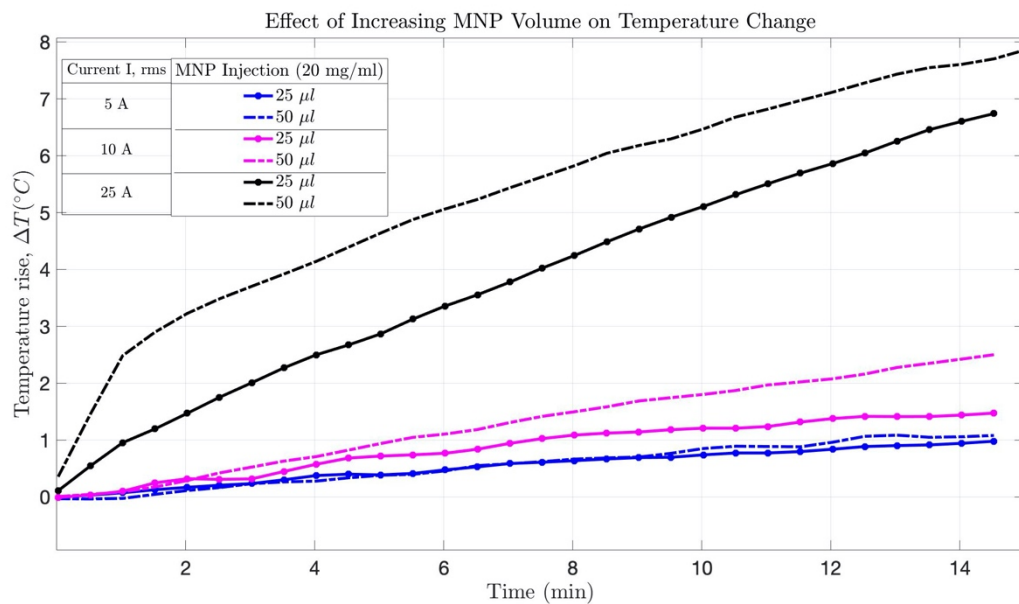


Figure 18: effect of increasing the MNP volume from 25 ul to 50 ul with 5, 10 and 25 A.

3.4 Trial with Optimal parameters

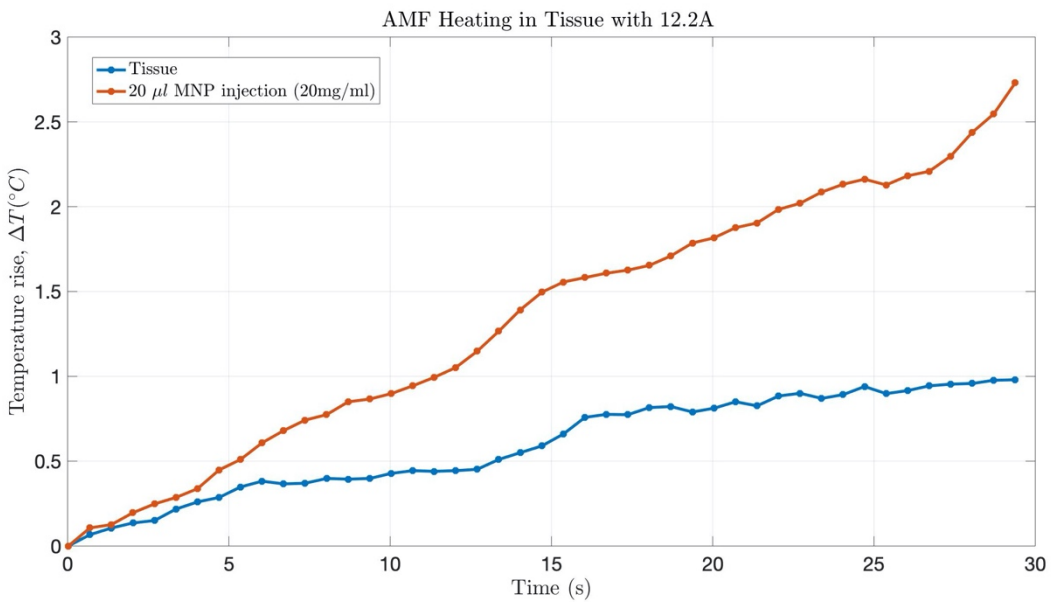


Figure 19: AMF heating in tissue with zero MNP injection and with 20 μ l MNP injection (20 mg/ml).

The applied $I_{rms} = 12.2A$ ($H=14.3$ kA/m).

Table 4: summary of the results for the trial with optimal parameters

Current I rms (A)	ΔT_{Tissue}	ΔT_{MNP} 20 μ l, (20 mg/ml)	R
12.2	1 $^{\circ}$ C	2.8 $^{\circ}$ C	2.8

3.5 Control Heating

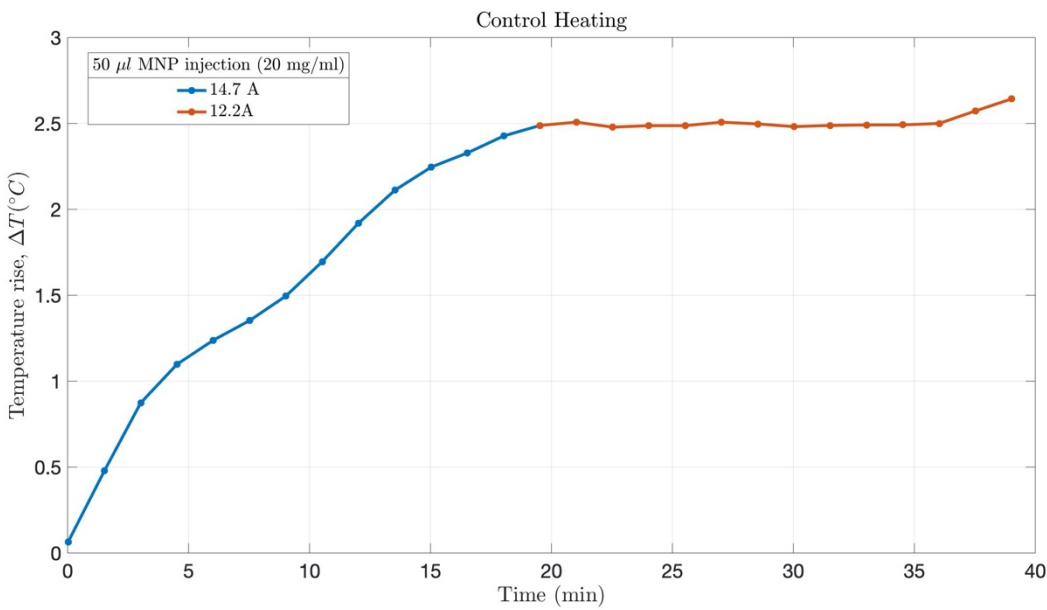


Figure 16: Trial for a control heating with 14.7A and 12.2A.

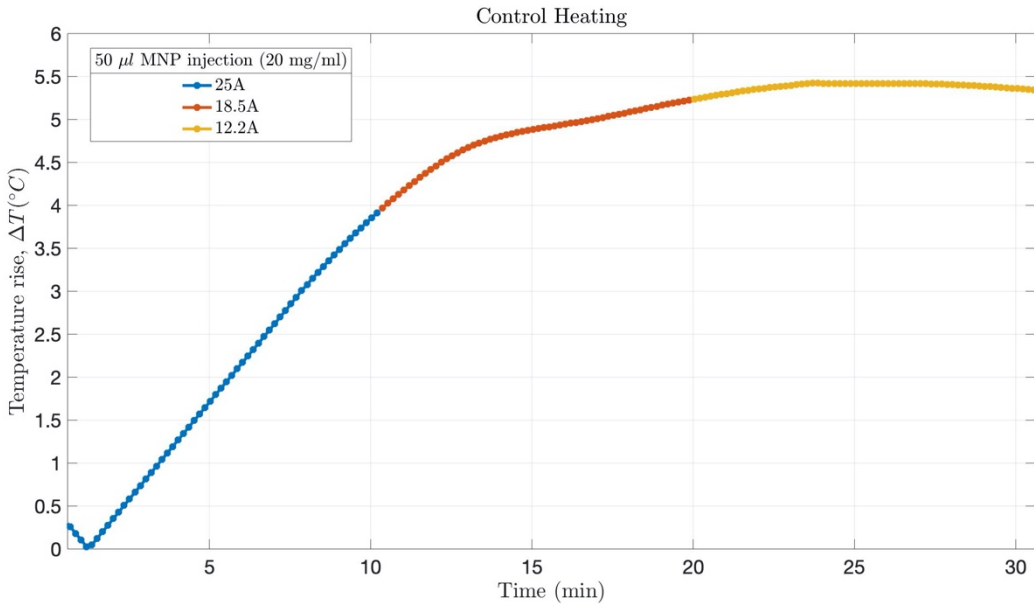


Figure 17: second trial for control heating with 25, 18.5 and 12.2 A.

3.6 Heating below the center of the loop

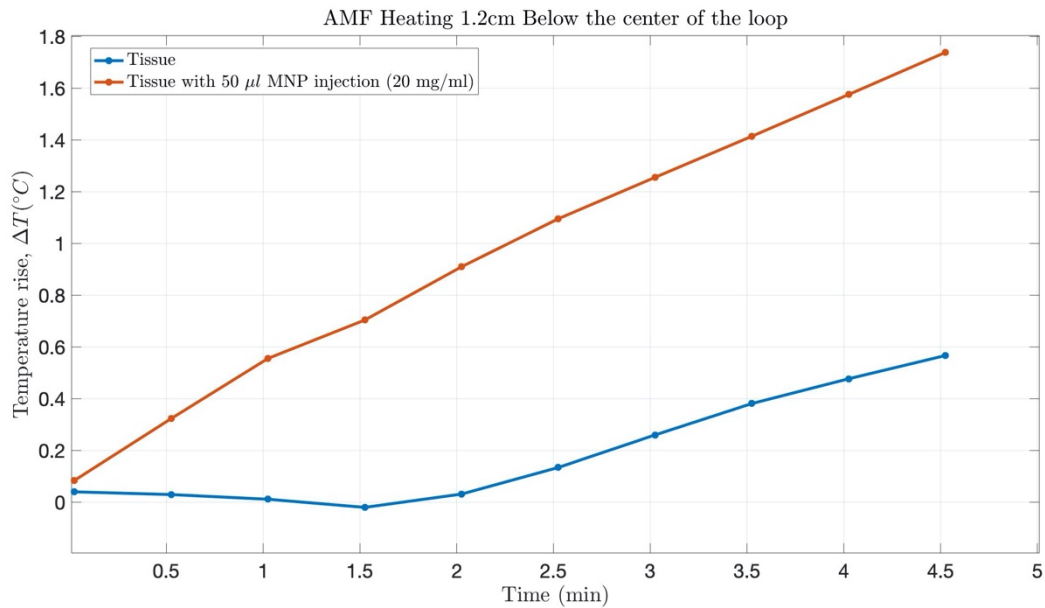


Figure 18: AMF heating in tissue 1.2 cm below the center of the loop with no MNP injection and with 50 μl MNP injection (20 mg/ml). $I_{rms} 25\text{A}$.

Chapter 4: Discussion

The effect of increasing the field strength H on heat generation were studied by applying currents from 5 to 25A where the calculated H around 5.8 to 29.5 kA/m.

It can be seen from Figure 4 that change in temperature increased as the applied field H increased. However, Figure 5 shows that nonselective heating results when $I_{rms} \geq 15$ A which represents high magnetic field strength $H \geq 17.7$ kA/m. figure shows that R decreases with increasing H, meaning higher non-specific heating occurs as H increased. Thus, the applied magnetic field strength should be limited to avoid nonspecific heating results from eddy current. Knowing the SAR linearly proportional to $\Delta T / \Delta t$, maximum SAR can be seen under the biophysical limitations (Rosensweig, 2002). Similar result observed by (Maxson & Mitchell, 2016) where Fe_3O_4 SIONPs with different diameters were exposed to magnetic field strength H from 15.1kA/m to 47.7 kA/m with a fixed frequency (f=194 kHz). It was found that SAR increased from 3.7 to 43.3 W/g which supports that SAR depends on H^2 as shown in Rosensweig model (Maxson & Mitchell, 2016).

Effect of MNP concentration was also investigated by heating 25 ul MNP in tissue with 5 and 20 mg/ml. It was observed that particles with 5mg/ml did not show any thermal rate at all applied magnetic field strength where the increase in T was even lower than the increase in T for tissue with no MNP injection. However, 20 mg/ml SIONPs shows a significant increase in T. Experimental results agree that it is important to have highly enough MNP concentration to cause a sufficient increase in T with minim applied AMF parameters (Maxson & Mitchell, 2016). Experimental result was done using collagen shows that the increase in T will be doubled as a result of doubling the MNP concentration(Suriyanto, Ng and Kumar, 2017).

Effect of MNP volume on thermal rate was also studied in section 3.3 and it was found that doubling the volume from 25 to 50 did not have a significant effect specially at low H and the reason for this was not fully understood.

Depending on the results presented here, optimal parameters were chosen to conduct an experiment for 30 min as shown in section 3.4.

Control heating was also studied, and it can be seen in section 3.5 that it is possible to increase the temperature to a therapeutic value and maintain it for a period of time. However, parameters chosen in Figure 17 will lead to nonselective heating, thus it is important to lower the applied magnetic field strength. As a result, feedback loop can be used to maintain the therapeutic temperature during the treatment.

Late experiment was done in order to investigate the possibility to lower the nonspecific heating caused by eddy current generation while using high current ($I_{rms} = 25A$, $H=10.5kA/m$). It can be seen that eddy current generation below the center of the loop is decreased. At high applied frequency, eddy current penetration in tissue is lower than eddy current penetration at low applied frequency, thus, heating below the center of the loop can be optimized to minimize eddy current generation and maximise the power loss by MNP.

4.1 Recommendations

Based on our result, it is recommended to keep the product of the applied magnetic field strength and frequency below a critical value. Our result is in consistence with Hergt et al., limitations where applied $Hf < 5 \times 10^9 A/ms$.

The following figure shows tissue heating with no MNP injection using 9.7 to 19.8A. It can be seen that heating tissue with 9.7A and 12.2A will increase the temperature for only 0.5 and 1°C

respectively. Also, after about 16 min of heating with 9.7 A, there is almost no increase in T. However, 12.2A, there is no more increase in T after about 20 min of heating unlike 14.7A and 19.8A which cause a significant increase in T. Thus, the calculated optimal H with f=394kHz is about 14 kA/m.

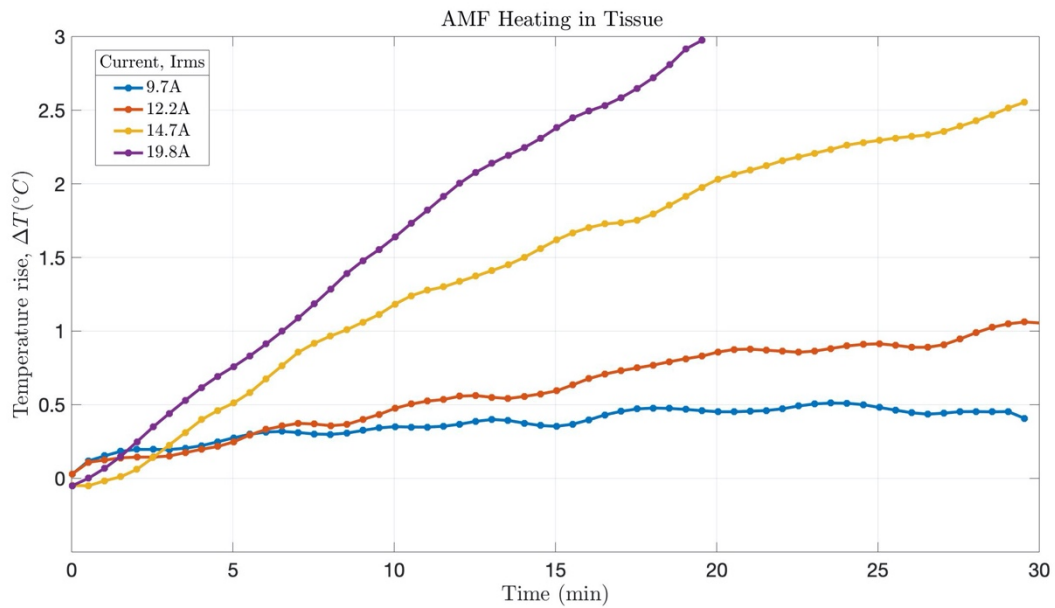


Figure 19: Heating tissue only with different current.

Chapter 5: Conclusion and Future studies

Magnetic nanoparticles Hyperthermia is one of the promising treatments that is under development. In general, hyperthermia is generating heat by increasing body temperature which leads to the death of cancer cells. Originally, heat was applied to the entire body or to a specific region of the body, however, the high temperature used will damage the healthy tissues causing many harmful side effects. Thus, delivering heat only to the cancer cells is required for hyperthermia to be an ideal cancer therapy. Recently, studying the field of magnetic nanoparticles (MNP) hyperthermia is at interest where alternating magnetic field (AMF) is used to induce heat generation. In order to deliver the minimum dose of magnetic nanoparticles (MNPs) to the desired location and producing the maximum amount of heat needed to kill cancer cells, optimal AMF strength and frequency, as well as optimal MNPs should be chosen. The optimal AMF can be adjusted by setting the product of $Hf < 5 \times 10^9 kA/ms$. MNPs prosperities depends on various of parameters that lead to variation in reported experimental results where different experiment shows different optimal parameters. Size, size distribution, coating concentration, and volume are some of many parameters that affect the MNP ability to dissipate heat. Increasing MNP concentration leads to higher heat generation which can optimize the treatment; however, it is important to keep it under the acceptable biological limit.

For future study, research on the effect of some MNP parameters needs to be done. Moreover, recent researches aim to find a method to lower eddy current generation to prevent nonselective heating and thus, higher AMF can be applied. One of the suggested methods is heating below the center of the loop; however, further investigations need to be done.

Chapter 6: References

- Atkinson, W. J., Brezovich, I. A. and Chakraborty, D. P. (1984) ‘Usable Frequencies in Hyperthermia with Thermal Seeds’, *IEEE Transactions on Biomedical Engineering*, BME-31(1), pp. 70–75. doi: 10.1109/TBME.1984.325372.
- Colombo, M. *et al.* (2012) ‘Biological applications of magnetic nanoparticles’, *Chemical Society Reviews*, 41(11), pp. 4306–4334. doi: 10.1039/c2cs15337h.
- Deatsch, A. E. and Evans, B. A. (2014) ‘Heating efficiency in magnetic nanoparticle hyperthermia’, *Journal of Magnetism and Magnetic Materials*, 354, pp. 163–172. doi: 10.1016/j.jmmm.2013.11.006.
- Dutz, S. *et al.* (2011) ‘Magnetic multicore nanoparticles for hyperthermia-influence of particle immobilization in tumour tissue on magnetic properties’, *Nanotechnology*, 22(26). doi: 10.1088/0957-4484/22/26/265102.
- Dutz, S. and Hergt, R. (2014) ‘Magnetic particle hyperthermia - A promising tumour therapy?’, *Nanotechnology*. IOP Publishing, 25(45). doi: 10.1088/0957-4484/25/45/452001.
- Estelrich, J. *et al.* (2015) ‘Iron oxide nanoparticles for magnetically-guided and magnetically-responsive drug delivery’, *International Journal of Molecular Sciences*, 16(4), pp. 8070–8101. doi: 10.3390/ijms16048070.
- Gas, P. (2011) ‘Essential facts on the history of hyperthermia and their connections with electromedicine’, *Przeglad Elektrotechniczny*, 87(12 B), pp. 37–40.
- Glöckl, G. *et al.* (2006) ‘The effect of field parameters, nanoparticle properties and immobilization on the specific heating power in magnetic particle hyperthermia’, *Journal of Physics Condensed Matter*, 18(38), pp. 2935–2949. doi: 10.1088/0953-8984/18/38/S27.
- Hegyi, G., Szigeti, G. P. and Szász, A. (2013) ‘Hyperthermia versus oncotherapy: Cellular

effects in complementary cancer therapy', *Evidence-based Complementary and Alternative Medicine*, 2013. doi: 10.1155/2013/672873.

Hergt, R. et al. (1998) 'Physical limits of hyperthermia using magnetite fine particles', *IEEE Transactions on Magnetics*, 34(5 PART 2), p. 37453754.

Hergt, R. et al. (2006) 'Magnetic particle hyperthermia: Nanoparticle magnetism and materials development for cancer therapy', *Journal of Physics Condensed Matter*, 18(38), pp. 2919–2934. doi: 10.1088/0953-8984/18/38/S26.

Hergt, R. and Dutz, S. (2007) 'Magnetic particle hyperthermia-biophysical limitations of a visionary tumour therapy', *Journal of Magnetism and Magnetic Materials*, 311(1 SPEC. ISS.), pp. 187–192. doi: 10.1016/j.jmmm.2006.10.1156.

Huang, H. S., & Hainfeld, J. F. (2013). Intravenous Magnetic Nanoparticle Cancer Hyperthermia. *International Journal of Nanomedicine*, 8, 2521–2532.
doi:10.2147/IJN.S43770

Jeyadevan, B. (2010) 'Present status and prospects of magnetite nanoparticles-based hyperthermia', *Journal of the Ceramic Society of Japan*, 118(1378), pp. 391–401. doi: 10.2109/jcersj2.118.391.

Jiles, D. (1991) *Introduction to Magnetism and Magnetic Materials*.

Kozissnik, B. et al. (2013) 'Magnetic fluid hyperthermia: Advances, challenges, and opportunity', *International Journal of Hyperthermia*, 29(8), pp. 706–714. doi: 10.3109/02656736.2013.837200.

Krishnan, K. M. et al. (2006) 'Nanomagnetism and spin electronics: Materials, microstructure and novel properties', *Journal of Materials Science*, 41(3), pp. 793–815. doi: 10.1007/s10853-006-6564-1.

- Li, C. H., Hodgins, P. and Peterson, G. P. (2011) ‘Experimental study of fundamental mechanisms in inductive heating of ferromagnetic nanoparticles suspension (Fe₃O₄ Iron Oxide Ferrofluid)’, *Journal of Applied Physics*, 110(5). doi: 10.1063/1.3626049.
- Ma, M. et al. (2004) ‘Size dependence of specific power absorption of Fe₃O₄ particles in AC magnetic field’, *Journal of Magnetism and Magnetic Materials*, 268(1–2), pp. 33–39. doi: 10.1016/S0304-8853(03)00426-8.
- Rhythm R. et al. (2016) ‘Impact of magnetic field parameters and iron oxide NP properties on heat HHS Public Access’, *Physiology & behavior*, 176(1), pp. 139–148. doi: 10.1016/j.physbeh.2017.03.040.
- Ondeck, C. L. et al. (2009) ‘Theory of magnetic fluid heating with an alternating magnetic field with temperature dependent materials properties for self-regulated heating’, *Journal of Applied Physics*, 105(7), pp. 103–106. doi: 10.1063/1.3076043.
- Pankhurst, Q. A. et al. (2003) ‘Applications of magnetic nanoparticles in biomedicine’, 36.
- Pankhurst, Q. A. (2006) ‘Nanomagnetic medical sensors and treatment methodologies’, *BT Technology Journal*, 24(3), pp. 33–38. doi: 10.1007/s10550-006-0072-3.
- Parmar, H. et al. (2015) ‘Size dependent heating efficiency of iron oxide single domain nanoparticles’, *Procedia Engineering*, 102, pp. 527–533. doi: 10.1016/j.proeng.2015.01.205.
- Reitan, N. K. et al. (2010) ‘Characterization of tumor microvascular structure and permeability: comparison between magnetic resonance imaging and intravital confocal imaging’, *Journal of Biomedical Optics*, 15(3), p. 036004. doi: 10.1117/1.3431095.
- Rosensweig, R. E. (2002) ‘Heating magnetic fluid with alternating magnetic field’, *Journal of Magnetism and Magnetic Materials*, 252(1-3 SPEC. ISS.), pp. 370–374. doi: 10.1016/S0304-8853(02)00706-0.

Salunkhe, A. B., Khot, V. M. and Pawar, S. H. (2014) ‘Magnetic Hyperthermia with Magnetic Nanoparticles: A Status Review’, *Current Topics in Medicinal Chemistry*, 14(5), pp. 572–594. doi: 10.2174/1568026614666140118203550.

Nanocomposix.eu. (2020). nanogold, nanosilver and other nanoparticles in exceptional quality. Retrieved from <https://nanocomposix.eu/>

Song, C. W. *et al.* (1984) ‘Implication of Blood Flow in Hyperthermic Treatment of Tumors’, *IEEE Transactions on Biomedical Engineering*, BME-31(1), pp. 9–16. doi: 10.1109/TBME.1984.325364.

Spaldin, N. A. (no date) *Magnetic Materials Fundamentals and Applications*.

Stigliano, R. V. *et al.* (2016) ‘Mitigation of eddy current heating during magnetic nanoparticle hyperthermia therapy’, *International Journal of Hyperthermia*, 32(7), pp. 735–748. doi: 10.1080/02656736.2016.1195018.

Suriyanto, Ng, E. Y. K. and Kumar, S. D. (2017) ‘Physical mechanism and modeling of heat generation and transfer in magnetic fluid hyperthermia through Néelian and Brownian relaxation: a review’, *Biomedical engineering online*, 16(1), p. 36. doi: 10.1186/s12938-017-0327-x.

Wang, E. C. and Wang*, A. Z. (2004) ‘NANOPARTICLES AND THEIR APPLICATIONS IN CELL AND MOLECULAR BIOLOGY’, *Library*, 6(1), p. 576. doi: 10.1039/c3ib40165k.NANOPARTICLES.

Wust, P. *et al.* (1994) ‘Hyperthermia in combined treatment of cancer’, *Neoplasma*, 41(5), pp. 269–276.

van der Zee, J. (2002) ‘Heating the patient: A promising approach?’, *Annals of Oncology*, 13(8), pp. 1173–1184. doi: 10.1093/annonc/mdf280.

Zhang, L. Y., Gu, H. C. and Wang, X. M. (2007) 'Magnetite ferrofluid with high specific absorption rate for application in hyperthermia', *Journal of Magnetism and Magnetic Materials*, 311(1 SPEC. ISS.), pp. 228–233. doi: 10.1016/j.jmmm.2006.11.179.